

Title No. 118-S55

Stochastic Finite Element Analysis of Shear-Critical Concrete Structures

by Mark D. Hunter, Anca C. Ferche, and Frank J. Vecchio

Stochastic simulation is used primarily as a basis for the resistance models in a reliability analysis, and it is often used to calibrate structural concrete building codes. This paper outlines the implementation of stochastic simulation techniques into a nonlinear finite element analysis framework. The stochastic modeling capabilities implemented include Monte Carlo (MC) sampling and Latin hypercube sampling for uncorrelated uniform sampling, uniform sampling with correlated random variables, and spatial variation using random field generation. Stochastic simulation was conducted for shear-critical beams containing no transverse reinforcement. The simulation results form the basis for a reliability analysis that computes the reliability index for the CSA A23.3-14 code. The calculated reliability index of 2.96 was lower than the target index of 3.5, indicating that the intended performance is not achieved for this type of element. As such, further investigation is required to assess the load factors and safety factors.

Keywords: finite element analysis; reinforced concrete; reliability analysis; stochastic simulation.

INTRODUCTION

Stochastic simulation is perhaps best understood in comparison with deterministic simulation. In a deterministic simulation, the goal of the selected model is to replicate a physical system. In the case of reinforced concrete, the Disturbed Stress Field Model¹ is a deterministic model for the analysis of reinforced concrete elements. It aims to provide an accurate stress-strain response for reinforced concrete treated as an anisotropic smeared cracked material. What categorizes this simulation as deterministic is the need to define the input parameters. If the input parameters are known, the model will produce an estimation of the physical behavior. In a stochastic simulation, the goal is to infer statistical data about an output quantity based on statistical knowledge of the system inputs. In the context of the analysis of reinforced concrete structures, the inputs under consideration are the spatial and global variability of the concrete and steel material properties, specified as a minimum compressive strength or yield strength, respectively.

Discrepancies between the properties of the specified structure and its actual in-situ properties can be significant. Thus, material resistance factors are included in limit state design. These material factors, however, are calibrated based on standard structural design procedures (that is, flexural strength of beams, sectional shear strength of beams, strut-and-tie models, and so on).²⁻⁴ When determining the reliability of structures with multiple potential failure modes and with complex geometry, the traditional method of treating the failure modes independently will create a different reliability coefficient for each failure mode. Any interaction

between failure modes or progressive failure modes (for example, shear failure after steel yielding but before the ultimate flexural response is reached) will not be captured. Thus, there is a need for advanced analysis tools that are capable of handling complex loading, material nonlinearity, and dynamic analysis which also can accommodate stochastic simulation. They can be particularly useful for field structural assessment scenarios when the determination of material properties is cumbersome or unfeasible.

In such cases, the assessment can be approached within a stochastic framework. Information on the distribution of concrete and steel material properties can be used to produce information on the distribution of the structure's expected strength and susceptibility to undesirable failure modes. Moreover, a stochastic simulation could be carried out to determine the reliability index for the structure; this reliability index can then be compared against code-recommended reliability indices to determine if the requirements of the local building code are met. In any case, a stochastic analysis provides a better measure of the confidence that should be associated with any calculated strength and failure mode.

In the case of reinforced concrete, it is well known that the concrete material properties exhibit a large variability.⁵⁻⁷ Nevertheless, the variability associated with existing infrastructure is not limited to the inherent material variability. There can be a large degree of uncertainty associated with any deteriorated structure. The extent, location, and implication of reinforced concrete deterioration is currently a topic of significant research.⁸⁻¹⁰ At the same time, there is much work to be done on the development of analysis tools that can capture concrete deterioration in a reliability framework.¹¹⁻¹⁶

A step toward adding to such tools is the focus of this work: the implementation of stochastic modeling capabilities within a nonlinear finite element analysis (NLFEA) program, VecTor2.¹⁷ Statistical models for concrete and steel material properties available in the literature have been identified and implemented within the proposed formulation. In addition, Monte Carlo (MC) and Latin hypercube sampling for uncorrelated uniform sampling, uniform sampling with random variables, and spatial variation using random field generation were implemented. Stochastic simulations were conducted on beam specimens with no transverse

ACI Structural Journal, V. 118, No. 3, May 2021.

MS No. S-2019-400.R3, doi: 10.14359/51730524, received June 23, 2020, and reviewed under Institute publication policies. Copyright © 2021, American Concrete Institute. All rights reserved, including the making of copies unless permission is obtained from the copyright proprietors. Pertinent discussion including author's closure, if any, will be published ten months from this journal's date if the discussion is received within four months of the paper's print publication.

reinforcement, and a reliability analysis was performed to determine the reliability index for the CSA A23.3-14 code.

The host program, VecTor2, employs a smeared, rotating crack model for concrete behavior based on the Disturbed Stress Field Model¹ and is suited for the analysis of two-dimensional reinforced concrete structures. The solution algorithm is based on an iterative, total-load, secant stiffness formulation with robust convergence characteristics. Mechanisms such as shear slip along crack interfaces, compression softening due to transverse cracking, confinement, and tension stiffening are among the several behavioral mechanisms considered explicitly. A broad range of models were implemented for each constitutive mechanism.

Central to the program's applicability to stochastic simulations is the minimal need for calibration. The default models available to represent the behavioral mechanisms have been extensively verified against various types of structures, thus making them a suitable choice for the majority of analyses. In addition, material characterization is especially straightforward. These traits make VecTor2 particularly useful for field structural assessment, scenarios in which access to mechanical properties of materials is limited. The addition of stochastic capabilities extends the application range of the program to structural reliability analysis in a framework that has shown to be suited for predictive type of analyses.

RESEARCH SIGNIFICANCE

In the case of reinforced concrete, reliability analysis has been used to calibrate building codes.²⁻⁴ The material resistance factors in the case of the CSA A23.3-14¹⁸ code, and the strength reduction factors in the case of the ACI 318-19¹⁹ code, are calibrated to achieve a code-level reliability. However, as a recent prediction competition²⁰ has shown, prediction of the shear strength of concrete beams with no transverse reinforcement still remains a challenging task. With such uncertainty, the calibration of resistance factors and load factors for building codes requires software that can provide a good deterministic prediction of structural behavior. NLFEA programs represent a viable option for the simulation of virtually any planar reinforced concrete element. The addition of stochastic simulation capabilities allows them to be used to create member resistance curves and thus be a useful tool in the assessment of safety and structural reliability for reinforced concrete members.

BASICS OF RELIABILITY ANALYSIS

Reliability analysis is the mathematical basis for the limit state design method. In a limit state design, the load that will act on the structure is predicted and factored by a prescribed value. Additionally, the resistance of each structural element is factored by either material resistance factors (CSA A23.3¹⁸) or strength reduction factors (ACI 318-19¹⁹). The derivation of these factors, for both loading and resistance, are the result of reliability methods. Adequate structural safety is determined by reducing the probability of failure of the structure.

In its simplest form, structural reliability is assessed by comparing the load effect S , and the resistance R , both described by known probability density functions f_S and f_R .

According to Melchers,²¹ the probability of failure p_f , for a structural element can be defined as

$$p_f = P(G(R,S) \leq 0) \quad (1)$$

where $G(R,S)$ is the limit state function; and in this case, it has the form $G(R,S) = R - S$.

The resistance and the load effect can be modeled using various probability distributions. In the particular case when R and S have normal distributions with the mean values μ_R and μ_S , and variances σ_R^2 and σ_S^2 , $G(R,S)$ has the mean and variance given by

$$\mu_G = \mu_R - \mu_S \quad (2)$$

$$\sigma_G^2 = \sigma_R^2 + \sigma_S^2 \quad (3)$$

The probability of failure of the structural element can be expressed as

$$p_f = P(G(R,S) \leq 0) = \Phi \left(\frac{0 - \mu_G}{\sigma_G} \right) = \Phi \left(\frac{-(\mu_R - \mu_S)}{\sqrt{\sigma_R^2 + \sigma_S^2}} \right) = \Phi(-\beta) \quad (4)$$

where $\Phi()$ is the standard normal distribution function; and $\beta = \mu_G/\sigma_G$ is the reliability index.²¹

The reliability index, β , is therefore a measure of safety; a higher value indicating a lower probability of failure. For a normal distribution, the reliability index can be calculated as

$$\beta = \frac{\mu_R - \mu_S}{\sqrt{\sigma_R^2 + \sigma_S^2}} \quad (5)$$

In general, the reliability analysis of a structure is more complex than the basic formulation presented previously. The load effect and the resistance may not be independent. In addition, both are functions of parameters that in turn may be random variables, such as the material properties, structural dimensions, and applied loads. Two approaches are typically used for the generalized reliability formulation²¹: the MC methods, and the First Order Second Moment methods. The procedure presented in this paper, however, considers the structural reliability of a single structural element. As such, a single resistance curve is determined through stochastic simulation, and a single load effect curve is assumed.

STOCHASTIC SIMULATION OF REINFORCED CONCRETE

MC methods have widely been used by researchers for assessing the structural reliability of reinforced concrete structures. MC simulations work by generating statistically independent samples that follow the distributions of each of the input parameters. The mathematical relationship describing the variable of interest is then computed for each

set of generated samples. This produces a set of outputs that can be statistically analyzed.

MC simulations have been employed to investigate the serviceability and strength behavior of concrete structural elements.¹¹⁻¹⁶ In what follows, the trends observed in the literature pertaining to input parameters, validation of theoretical model, and structural behavior are summarized.

The input parameters for stochastic simulations most often considered in the literature were the concrete material properties, the steel material properties, and the dimensional properties. The concrete material properties modeled included the compressive strength, the modulus of elasticity, and the tensile strength. In studies concerned with long-term effects, statistical properties were considered for the creep and shrinkage coefficients. The statistical properties most commonly considered for reinforcing steel were the modulus of elasticity, the nominal cross-sectional area of steel, and the yield strength.

The variation in assumed dimension for a given structural element is less important to the current work because a finite element approach will be taken using two-dimensional membrane elements.

In all of the MC simulations reviewed,¹¹⁻¹⁶ a theoretical model was proposed to describe the parameter of interest. Despite the large disparity in complexity between studies, most of the studies verified the proposed theoretical model against deterministic results in the literature. It is recommended that all MC simulations validate the theoretical model against experimental results obtained from the literature.

Most of the simulations reviewed were flexural elements.¹¹⁻¹⁵ In cases where shear was considered as a failure mode,¹⁶ the stochastic parameters were typically applied to the simplified empirical shear equations. Such an approach likely does not capture the transition in failure mode or the interactions between shear behavior and flexural behavior. Stochastic simulations of shear-critical members, disturbed regions, or any other structural element that deviates from the simplified equations requires more advanced analysis tools. Strut-and-tie models have been shown to represent a lower bound estimate of the strength of such structural elements, and it would thus not be prudent to use such techniques for reliability studies. A requirement then exists to study the reliability of such structures with advanced and accurate finite element models. Such an approach is proposed in this article.

SOFTWARE FORMULATION

Statistical models of material properties

The statistical models used in a stochastic simulation of reinforced concrete must be selected such that the distributions are representative of in-place variability. Consideration must be given to the age and location of the structure, both of which can influence the statistical distributions of the material parameters. Four statistical models for concrete material properties and two for steel were identified from the literature and implemented within the proposed formulation. For the material properties of concrete, the variability of the compressive strength, the tensile strength, and the modulus

Table 1—Selected statistical models

Parameter	Statistical models
Concrete	
Compressive strength	Mirza et al. ⁵ Bartlett and MacGregor ^{6*} Nowak and Szerszen ² Unanwa and Mahan ⁷
Modulus of elasticity	Mirza et al. ⁵ Hybrid* Mirza ⁵ + CSA
Tensile strength	Mirza et al. ⁵
Steel	
Yield strength	Mirza and MacGregor ²² Nowak and Szerszen ^{2*}
Ultimate strength	Mirza and MacGregor ^{22*}
Modulus of elasticity	Mirza and MacGregor ^{22*}

*Recommended default model.

of elasticity were considered. For the reinforcement, statistical models for the steel yield strength, the ultimate strength, and the modulus of elasticity were included. A summary of the statistical models selected for the proposed procedure is presented in Table 1.

The models proposed by Mirza et al.⁵ (for concrete) and Mirza and MacGregor¹² (for steel) have been widely employed in stochastic simulation and in the calibration of building codes.¹¹⁻¹⁴ Further work by Bartlett and MacGregor⁶ provided more detailed models that were subsequently used in building code calibration. Nowak and Szerszen² provided an updated and improved database for the statistical properties of steel and concrete that was used in the calibration of ACI 318-19 Code.¹⁹ Most recently, a study by Unanwa and Mahan⁷ provided results that agree with previous literature and offer updated models for temporal effects on the strength of concrete.

Random variable generator

A stochastic variable generator was created that uses the implicit function in the Fortran Library and generates random samples of normal, lognormal, gamma, and beta distributions. These distributions are then used to generate random samples for the concrete and steel material properties. The user selects which distribution to use for stochastic analysis. A variety of statistical models from the literature are implemented, as well as the ability to consider user-defined statistical properties. The subroutine then builds a matrix that stores the statistical parameters for each selected distribution as well as an identifier that indicates which sampling function to call. Once a sample is generated for each distribution, the ratio between the specified value and the sampled value is taken and assigned as a modification factor to each material property.

It is often useful to generate samples of nonuniform random variables. In the case of the normal and lognormal random variable sampling, the Box-Muller Method (Graham and Talay²³) was adopted to generate a sample of a normally distributed random variable. The gamma random variable generator implementation is based on the Marsaglia

and Tsang²⁴ method. Additional details on the nonuniform random variable sampling method implemented can be found in Hunter.²⁵ Appendix A* summarizes the validation procedure for the random variable generator.

Analysis types

Monte Carlo sampling—MC sampling involves basic random number generation for any of the selected distributions. The user is able to select a distribution for the concrete compressive strength, the concrete tensile strength, the concrete elastic modulus, the steel yield strength, the steel ultimate strength, and the steel elastic modulus. The models recommended and set as the default distributions are shown in Table 1.

The selected models are not specific to MC sampling but are recommended for all stochastic simulations. Note that for the concrete tensile strength and elastic modulus, the CSA A23.3¹⁸ relationships for the modulus of elasticity and tensile strength are substituted. This was considered more representative of modern-day concrete than the original statistics proposed by Mirza et al.⁵ The selection of Mirza et al.⁵ models for the tensile strength and modulus of elasticity reflects the understanding that a contemporary database of those parameters has not recently been compiled for Canadian concrete.

Latin hypercube sampling—LHS was first proposed by McKay et al.²⁶ as a method for reducing the number of required simulations. It has been further developed and employed for stochastic simulation with finite elements.²⁷ This method is able to produce samples that cover the entire distribution range but reduces the computational effort when compared with full factorial design.

The LHS technique is advantageous when the computation time for each simulation is long. Some researchers estimate that satisfactory results can be obtained with fewer than 50 simulations (Vořechovský and Novák²⁸). Nevertheless, between 50 and 100 simulations are recommended when LHS is employed. Further details on the LHS implementation are provided in Appendix B and by Hunter.²⁵

Correlated sampling—Multiple empirical functions have been developed to express the relationships between the compressive strength of concrete and its tensile strength or elastic modulus. These relationships are based on regression analysis of experimental data. If concrete compressive strength exhibits variability for a given specified strength, it is reasonable to assume that a correlation exists between the compressive strength and the corresponding tensile strength and modulus of elasticity. Correlated sampling can thus serve as a useful tool for the sampling of reinforced concrete material properties.

Correlated sampling is performed during individual simulations using the same approach as with the basic MC sampling method. The method can be extended to introduce correlation into LHS. When compared with correlated MC samples, the correlated Latin hypercube (CLH) samples

provide a marginal improvement on the estimate of the correlation matrix and a large improvement on the estimate of the mean and standard deviation.²⁵

Random field generation

Random variations of material properties occur not only from structure to structure, but also within a structure. In the case of a finite element simulation, each element can be assumed to take on a random value of a material property. However, the elements cannot be assigned a truly random value. It is logical to assume that a correlation exists between adjacent elements, creating gradient-like transitions. Thus, a method is required to generate stochastic samples of spatially distributed randomness that captures the spatial correlation between adjacent finite elements. This can be done using random fields.

Random fields are spatially correlated stochastic samples that follow a specified distribution. The Gaussian random field is the model adopted in the proposed procedure. The Karhunen–Loeve transform (KL transform), also called the orthogonal transform, is the most widely used method for generating random fields (Choi et al.²⁹). The transformation takes the form of an eigenvalue problem where each of the transformed random variables can be generated independently. A comparison between independently generated element values and spatially correlated random values is shown in Appendix C.

A random field requires three parameters: the number of included eigenvalues, the random field variance, and the correlation length. The recommended number of eigenvalues varies depending on the correlation length. It has been found that selecting 80 eigenvalues is adequate in generating random fields for the correlation lengths typically observed in concrete, as discussed by Hunter.²⁵ The correlation length describes the distance in which two elements become completely uncorrelated. A review of the literature suggests that a correlation length of 800 to 1200 mm (31.5 to 39 in.) is recommended for stochastic simulations.²⁵ The current implementation produces a random field with a mean of zero and a variance equal to the specified variance; however, this random field is then scaled to meet the global distribution for concrete. As a result, until the random field data implementations are expanded to include non-Gaussian random fields, the random field variance parameter should always be specified as 1.0.

RELIABILITY OF SHEAR-CRITICAL BEAMS WITH NO TRANSVERSE REINFORCEMENT

VecTor2 professional factor

There has always been an understanding that despite the best efforts of structural engineers, the simulation of structural behavior is only an approximation to reality. It is important to quantify and understand how analysis tools used for reliability analysis are representative of reality. The professional factor in this study is defined as an additional random variable that captures the uncertainty derived from modeling. For VecTor2, the NLFEA program used, this notion is incorporated into the material resistance model as a product between the specific professional factor, the

*The Appendix is available at www.concrete.org/publications in PDF format, appended to the online version of the published paper. It is also available in hard copy from ACI headquarters for a fee equal to the cost of reproduction plus handling at the time of the request.

fabrication factor, and the predicted resistance model. This is reflected in Eq. (6)

$$R = R_n \times M \times P \times F = R_{VT2} \times P \times F \quad (6)$$

where R_n is the nominal resistance; M is the material property parameter; $R_{VT2} = R_n \times M$ is taken as the result of the stochastic simulation; P is the professional factor; and F is the fabrication factor. The professional factor, P , is defined as the ratio between the experimental and predicted capacity, P_{Exp}/P_{VT2} .

VecTor2 is a general-purpose finite element program; as such, it will model different structures with varying degrees of accuracy. For example, consider the statistics published by Vecchio et al.³⁰ The means for the ratios of calculated-to-experimental strengths (P_{VT2}/P_{Exp}) for beams, shear walls, and panels (that is, the bias factors) were reported to be 1.000, 1.011, and 1.022, respectively. Similarly, the coefficients of variation for those elements were reported to be 5.3%, 20.3%, and 9.6%, respectively. Thus, although all three examples show a bias factor of approximately 1.0, the coefficient of variation due to model uncertainty varies significantly depending on which structural element is selected for modeling. Note that these reported numbers were calculated for (P_{VT2}/P_{Exp}); however, in this study the inverse of the ratio is required and used as the professional factor.

In the current study, shear-critical beams with no transverse reinforcement are being modeled. To assess the professional factor for VecTor2 when considering shear-critical beams, a large number of beams must be modeled. The database published by Reineck et al.³¹ contains a total of 744 shear-critical beams that were tested under a one-point or two-point bending test. The total of 744 was reduced to a subset of 680 by removing all T-beams. The set of beams was additionally refined by removing all beams without sufficient and reliable information needed to model the beams in VecTor2. This resulted in a set of 371 beams remaining.

For the analysis of the selected data, a few simplifying assumptions were made; the first was that the bottom steel reinforcement could be modeled as a single layer of reinforcement with a centerline equal to the centroid of the reinforcement. Each beam was assumed to be perfectly symmetric, and, thus, only half of the beam was modeled around the plane of symmetry. It was further assumed that the reinforcement was perfectly bonded to the concrete. This assumption is considered to be reasonable because only shear tests with deformed reinforcing bars were selected. Lastly, the predicted load-deflection response was found to be sensitive to the assumed maximum crack spacing. As a result, a consistent estimation of the maximum crack spacing based on the CEB-FIB³² code was assumed to govern both directions, as per Eq. (7)

$$s_{mx} = 2 \left(c_x + \frac{s_x}{10} \right) + 0.25k_1 \frac{d_{bx}}{\rho_x} \quad (7)$$

where c_x is the maximum distance from the reinforcement; s_x is the horizontal spacing of the longitudinal reinforcement;

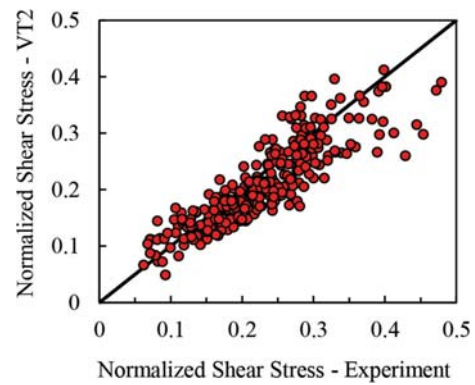


Fig. 1—Comparison of experimental and theoretical normalized shear stresses.

d_{bx} is the diameter of the longitudinal reinforcing bars; and ρ_x is the longitudinal reinforcement ratio. The parameter k_1 is taken as 0.4 for deformed reinforcing bars.

A representative finite element model is shown in Appendix D, Fig. D(a). For all specimens analyzed in this study, four-node plane stress rectangular elements were used to model the concrete component and the bearing plates, whereas the reinforcement was represented by truss bar elements. For each beam, a unique structure file and two load case files were required to properly define the finite element model for the beam. An automated preprocessor was developed to read the input information for each beam and generate the structure file and the load case files required for analysis. In addition, a MATLAB script was developed to run each of the executables, thereby additionally increasing the automation. Finally, a postprocessor was developed in MATLAB to visualize the results. The automated process was not without errors; of the selected 371 beams, 53 of the automatically generated meshes produced errors when running. As such, these 53 models were excluded from the reported results. This was considered acceptable because the sample size of 318 is considered sufficient to estimate the professional factor. Appendix E summarizes the dimensions of the beam specimens as well as the simulation results.

A plot showing the normalized shear stress $V/bd\sqrt{f'_c}$ for the experimental data versus the simulated data is shown in Fig. 1. It can be seen from the plot that there is significant scatter in the prediction of the shear strength using VecTor2. The data do appear to capture the behavior of all of the beams reasonably well. Additionally, the majority of the tests fall under the equal ratio and are thus conservative predictions of the shear strength.

The professional factor P , is defined in Eq. (8) as the ratio between the experimental (V_{Exp}) and predicted peak load (V_{VT2}). This ratio was calculated for each simulation and analyzed as a set of data. The calculated professional factors were found to be normally distributed with a mean of 1.106 and a coefficient of variation of 0.183. The mean value of the professional factors is referred to as the bias factor. A histogram showing the normal distribution fit is shown in Fig. 2. A χ^2 goodness-of-fit test and a KS test were performed. Both tests confirmed the goodness of fit and provided p -values of 0.172 and 0.372, respectively. Therefore, the professional factor can be modeled as a normal distribution.

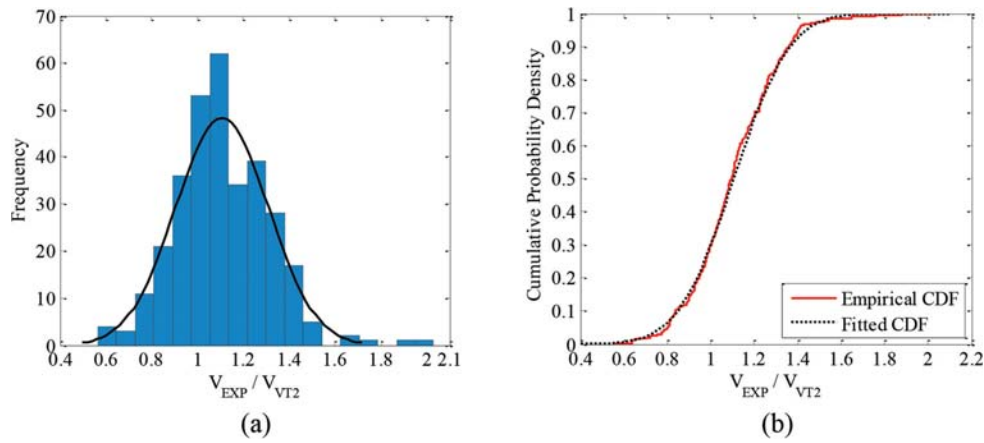


Fig. 2—(a) Histogram; and (b) fitted distribution for VecTor2 professional factor.

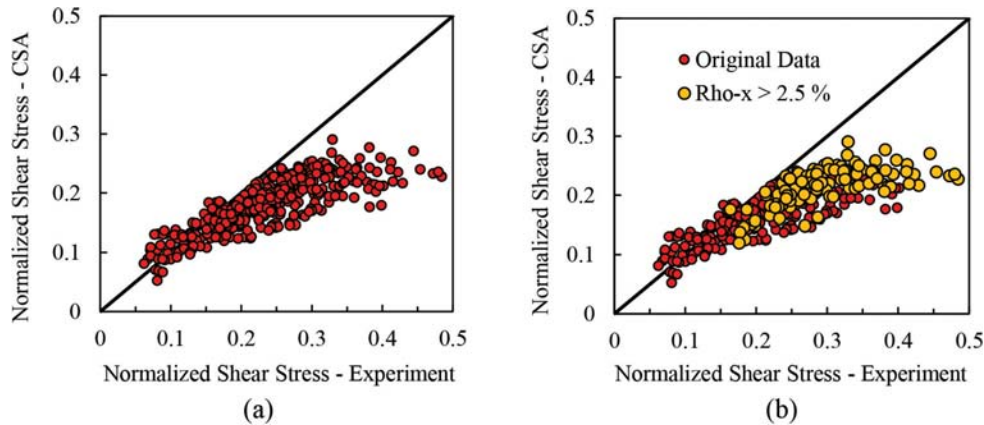


Fig. 3—CSA A23.3 predictions for shear strength versus experimental results: (a) original data; and (b) disaggregated data with $\rho_x \geq 2.5\%$.

$$P = V_{Exp}/V_{VT2} \quad (8)$$

The uncertainty attributable to testing procedures and the differences between assumed and actual specimen properties are incorporated into the computation of the professional factor using the same method as that by Mirza and MacGregor.¹² The coefficient of variation for the professional factor, denoted as V_p , is calculated using Eq. (9) as equal to 0.174.

$$V_p = \sqrt{V_{t/c}^2 - V_{test}^2 - V_{spec}^2} \quad (9a)$$

$$V_p = \sqrt{(0.183)^2 - (0.03)^2 - (0.045)^2} = 0.174 \quad (9b)$$

where $V_{t/c} = 0.183$ is the coefficient of variation obtained from the comparison of experimental-to-calculated strengths; V_{test} represents uncertainties related to testing procedures such as load recording and is recommended by Mirza and MacGregor¹² to be taken as 0.030; and V_{spec} represents uncertainties related to measured dimensions and in-batch variations in material properties and is recommended¹² to be taken as 0.045.

The analysis of the selected test data was repeated with the CSA A23.3¹⁸ code. These analyses were done not for the purpose of developing a professional factor for the

CSA A23.3¹⁸ code but rather to compare the results with VecTor2. The CSA code and VecTor2 are both implementations based on the modified compression field theory.³³ The CSA code simplifies the original Modified Compression Field Theory,³³ and it is calibrated for analysis of flexural elements.³⁴ VecTor2 uses the Disturbed Stress Field Model¹ and expands on the Modified Compression Field Theory³³ by including shear slip along crack surfaces. The results for the CSA code are shown in Fig. 3(a).

It can be seen that for most of the test results, the CSA code is conservative. It becomes partially unconservative for specimens that develop lower shear stress. However, given the overall scatter, it is reasonable to assume that the mean value of the CSA equations are good predictors of the shear strength and that the variability observed in the figure is acceptable given the simplicity of the model. It is worth noting that VecTor2 also experiences significant scatter in these regions, although it does not appear to have an unconservative bias.

It is also evident in Fig. 3(a) that the CSA code conservatively predicts strengths for tests that can develop high shear stress. During the early experimental exploration of the shear strength of concrete, researchers often designed beams with large tensile reinforcement to induce a shear failure. However, it was not understood at the time that the presence of large amounts of longitudinal reinforcement reduces the overall tensile strains in the shear zone and thus

Table 2—Properties of selected specimens for Toronto Size Effect series

Specimen	b , mm	d , mm	a/d	f'_c , MPa	A_g , mm	f_y , MPa	ρ_{Long} , %
BN 50	300	450	3.00	37	10	483	0.81
BN 100	300	925	2.92	37	10	550	0.76
YB 2000	300	1890	2.86	33.6	10	447	0.74
PLS 4000	250	3840	3.13	39.4	14	573	0.656

Note: b is width; d is effective depth; a is shear span; f'_c is concrete compressive strength; A_g is maximum aggregate size; f_y is longitudinal reinforcement yield strength; ρ_{Long} is longitudinal reinforcement ratio; 1.0 mm = 0.04 in.; 1 MPa = 145 psi.

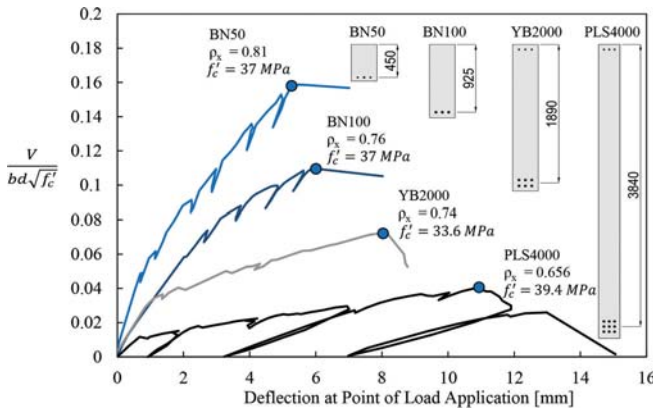


Fig. 4—Normalized shear stress response for selected beams: BN50³⁵; BN100³⁵; YB2000³⁶; and PLS4000.³⁷ (Note: Units in mm; 1.0 mm = 0.04 in.)

strengthens the shear capacity of such beams. When the results are disaggregated, the effect of the reinforcing ratio on the CSA predictions becomes clear. Figure 3(b) shows the disaggregated results for the CSA predictions. The data has been separated into two categories: longitudinal reinforcing ratio greater than 2.5% or less than 2.5%. The 2.5% was selected as a large, yet realistic, reinforcing ratio. It is clear from the figure that most of the tests poorly captured by the CSA code have a reinforcement ratio above 2.5%.

Toronto Size Effect series

In what follows, a case study is presented that highlights the potential applications of the implemented software pertaining to stochastic simulation. A series of deep beams with no transverse reinforcement are simulated, and their reliability is discussed.

The size effect in shear is a well-documented phenomenon that has been incorporated into several design codes around the world (for example, CSA A23.3, ACI 318-19, AASHTO, Eurocode 2). The size effect in most cases is an additional parameter that is applied to the shear strength. This results in diminishing returns on the concrete contribution to shear strength when the depth of the beam increases. It is unclear how the size effect affects the computed reliability of the reinforced concrete beam elements.

Four reinforced concrete beams, tested at the University of Toronto, were selected from the literature for stochastic simulation.³⁵⁻³⁷ The first two beams, BN50 and BN100, tested by Podgorniak-Stanik,³⁵ had depths of 500 mm (19.7 in.) and 1000 mm (39.4 in.), respectively. The third beam, YB2000, tested by Yoshida,³⁶ had a depth of 2000 mm (78.4 in.). The last beam, PLS4000, was a slab strip tested by Quach³⁷ and

had a depth of 4000 mm (157.5 in.). Beams BN50, BN100, and YB2000 had a thickness of 300 mm (11.8 in.). The slab strip PLS4000 had a thickness of 250 mm (9.8 in.). The properties of each beam are summarized in Table 2. A plot of the normalized shear stress at the critical section versus deflection at the point of load application for each beam is shown in Fig. 4.

Deterministic analysis—In modeling BN50, a finite element mesh with a total of 20 elements through the thickness and an average element size of approximately 25 x 25 mm (1.0 x 1.0 in.) was used. The finite element mesh is shown in Appendix D, Fig. D(b). The steel bearing plates for the applied load were modeled by one layer of steel plate material and one layer of bearing material. The longitudinal reinforcing steel was modeled using truss elements. A maximum crack spacing of 693 mm (27.3 in.) was determined using Eq. (7).

Specimen BN50 exhibited a bilinear response and a brittle failure at an ultimate load of 261 kN (58.7 kip) and a deflection of 5.6 mm (0.22 in.). The failure was the result of a large shear crack opening up. The finite element model was able to capture the experimental response of the specimen reasonably accurately. The predicted ultimate load and displacement were 266 kN (59.8 kip) and 4.8 mm (0.19 in.), respectively. A plot of the experimental load-deflection response and the finite element prediction is shown in Fig. 5(a). The finite element model tends to overestimate the precracked stiffness of the response but produces a reasonable estimate for the postcracked stiffness of the experimental response. The predicted load was 1.9% larger compared to the experimental measured one.

For specimen BN100,³⁵ a finite element mesh of 7194 elements was constructed. A total of 21 elements were used through the depth of the beam with an average element size of approximately 50 x 50 mm (2.0 x 2.0 in.). The finite element mesh was similar to the one built for specimen BN50. A maximum crack spacing of 1226 mm (48.3 in.) was determined using Eq. (7).

The onset of failure occurred at a peak load of 370 kN (83.2 kip) and a peak deflection of 5.87 mm (0.23 in.). The finite element model predicted a peak load of 406 kN (91.3 kip) and a peak deflection of 5.98 mm (0.24 in.). This was in reasonably good agreement with the experimental results, with the peak load calculated to be 9.7% larger than the experimental one. A comparison of the experimental and predicted load-deflection response is shown in Fig. 5(b). Note that the initial stiffness predicted by the finite element model is stiffer than the experimental results. It is possible that the beam was precracked due to accidental loading

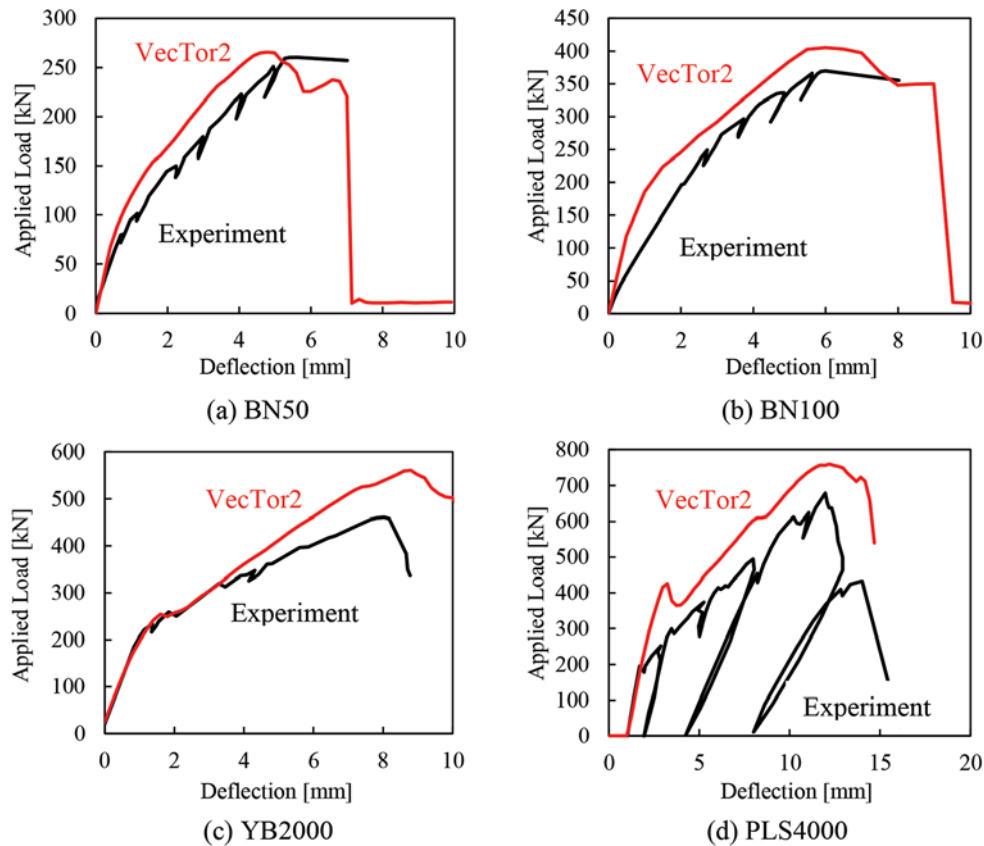


Fig. 5—Experimental versus FEA results for: (a) BN50; (b) BN100; (c) YB2000; and (d) PLS4000 specimens. (Note: 1.0 mm = 0.04 in.; 1 kN = 0.225 kip.)

before testing or due to restrained shrinkage. However, because the peak response is modeled reasonably well and the initial stiffness of the other three specimens was in good agreement with the experimental results, this discrepancy is not considered important to this study.

Specimen YB2000 was tested by Yoshida³⁶ as part of a series of deep beam tests with varying amount of transverse reinforcement. A maximum crack spacing, determined using Eq. (7), was calculated to be 2181 mm (85.9 in.). The finite element model was able to produce reasonable predictions of the initial stiffness and cracking load for the YB2000 specimen. However, the postcrack stiffness, ultimate load, and deflection at ultimate were overestimated. The finite element model predicted a failure load of 562 kN (126.3 kip) with a deflection of 8.79 mm (0.35 in.). A comparison of the finite element and experimental load-deflection curves is presented in Fig. 5(c). Although the finite element prediction overestimates the experimental response by approximately 22% in regard to ultimate strength, it was considered reasonable enough to continue with stochastic simulation.

The specimen PLS4000 tested by Quach³⁷ was a deep beam specimen meant to represent a slice of a deep slab foundation. The mesh used for simulation is shown in Appendix D, Fig. D(c). A maximum crack spacing of 4035 mm (158.9 in.) was selected based on Eq. (7). Similar to specimen YB2000, this test was designed to have two shear tests in one specimen. The west span contained 20M T-headed shear reinforcement, with the cross-sectional area of 300 mm² (0.465 in.²), spaced at 1500 mm (59 in.). The east span contained no transverse reinforcement and is thus

the subject of this study. The experimentally measured peak load was 685 kN (154 kip) with a peak deflection of 12 mm (0.47 in.). The finite element analysis predicted a peak load of 761 kN (171 kip) and a deflection at peak load of 12.2 mm (0.48 in.). The calculated peak load was 11% larger than the experimentally measured one. A comparison of the experimental and finite element load-deflection curves is shown in Fig. 5(d). Illustrated in Appendix F is the comparison between the simulated versus observed crack patterns at failure for Specimen PLS4000. The crack pattern was captured reasonably well, with failure being initiated by the development of a large diagonal crack both analytically and experimentally.

All four deterministic finite element models were reasonably successful in predicting the experiments, given the high degree of scatter typically obtained from various other modeling procedures and software for such elements.³⁷ For Specimens BN50 and BN100, the transition between the uncracked response and cracked response was not clearly captured experimentally; however, the experimental peak loads and displacements were in good agreement with the analytical ones. For YB2000 and PLS4000, the precracked stiffnesses were accurately captured. A good match for the transition between cracked and uncracked stiffness was obtained for Specimen YB2000. However, for PLS4000, the cracking load was overestimated. In all cases, a reasonable agreement between the experimental and analytical results was obtained for the postcracked stiffness, the peak load, and deflection. Note that all analyses were done using

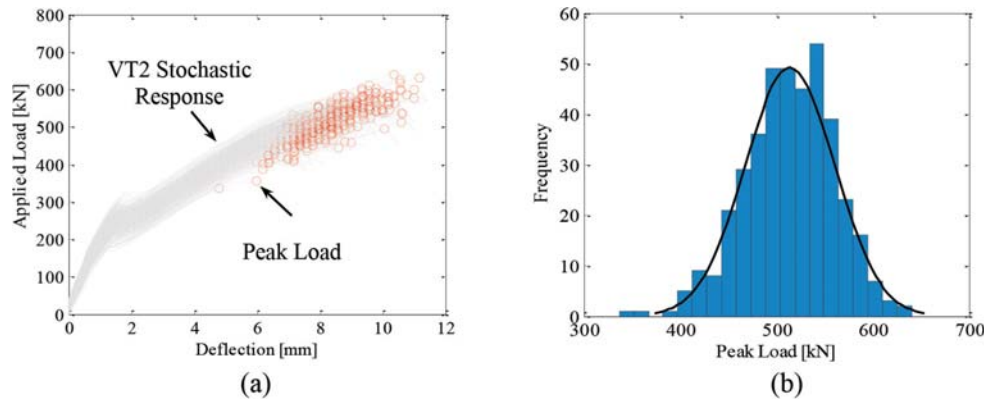


Fig. 6—Example of stochastic simulation results for Specimen YB2000: (a) simulated load-deflection; and (b) statistical distribution of peak load. (Note: Units in mm; 1.0 mm = 0.04 in.; 1 kN = 0.225 kip.)

Table 3—Stochastic simulation input properties for concrete

Variable	Model	Mean value, MPa	Standard deviation, MPa	Coefficient of variation, %
Compressive strength $f'_c = 30$ MPa	Bartlett and MacGregor ⁶	38.57	7.14	18.6
Tensile strength $f'_t = 1.81$ MPa	Modified Mirza et al. ⁵	1.81	0.23	12.7
Modulus of elasticity $E_c = 25,084$ MPa	Modified Mirza et al. ⁵	25,084	2006.7	8.0

Note: 1 MPa = 145 psi.

Table 4—Stochastic simulation results

Specimen	No. of simulations	Statistical distribution	$\mu_{Peak Load}$, kN	$\lambda = \mu_{Peak Load}/R_{CSA}$	Simulated COV	p -value χ^2/KS
BN 50	200	Normal	235.0	1.200	0.116	0.563/0.342
BN 100	300	Normal	324.4	1.040	0.092	0.932/0.475
YB 2000	398	Normal	513.9	1.101	0.091	0.464/0.536
PLS4000	175	Normal	652.3	1.226	0.112	0.365/0.134
			Average	1.142	0.103	

default models and parameters, and no attempt was made to fine-tune the analyses.

In addition, the CSA A23.3¹⁸ code was used to determine the shear strength of the selected specimens. A plot of the code predictions is shown in Appendix G. In this plot, the shear is generalized into a 1.0 m (39.4 in.) wide section. Each of the experimental results for the selected specimens is plotted on the figure. These results were determined as the summation between the applied shear and the shear due to the self-weight of the specimen.

Stochastic simulation results—Stochastic simulation was conducted for the selected specimens from the Toronto size effect series. The number of simulations for each specimen varied based on computation time. Each simulation consisted of a random field using LHS for the specified concrete strength, assumed to be 30 MPa (4350 psi). The steel properties were assumed to be deterministic. This was done because the mechanical properties of the longitudinal reinforcement have limited influence on the behavior of shear-critical beams with no transverse reinforcement. The strain in the steel is influenced only by the steel modulus of elasticity, which exhibits only small variability. The stochastic analysis parameters for concrete are outlined in Table 3.

The distributions from Table 3 represent the global distributions. However, as discussed previously, the local

spatial variation is lower. For the purpose of this study, the spatial variation due to the random fields was based on the measured properties of PLS4000.³⁷ A correlation length of 1200 mm (47.2 in.) and the random field coefficient of variation of 5.0% were selected. The simulation results produce a series of load-deflection curves. A typical plot of the stochastic simulation results is plotted in Fig. 6(a). The peak loads obtained from the stochastic simulations can then be analyzed as a set of random data. A statistical distribution is fitted to the results of each simulation. Figure 6(b) shows an example of the distribution of the peak load for specimen YB2000. Additional details on the stochastic simulation results are discussed by Hunter.²⁵

The results of each simulation were determined to be normally distributed. A χ^2 goodness-of-fit test and a KS test were used to assess the fits. The p -values for each statistical test are shown in Table 4. The average bias factor and coefficient of variation are also presented in the table. These average values are used in the reliability analysis.

Each of the stochastic simulations showed a mean value very close to the nominal resistance calculated by the CSA A23.3 general method. A plot of the general method compared with the stochastic simulation results is presented in Fig. 7. The simulation results were transformed from applied peak load to shear force per meter.

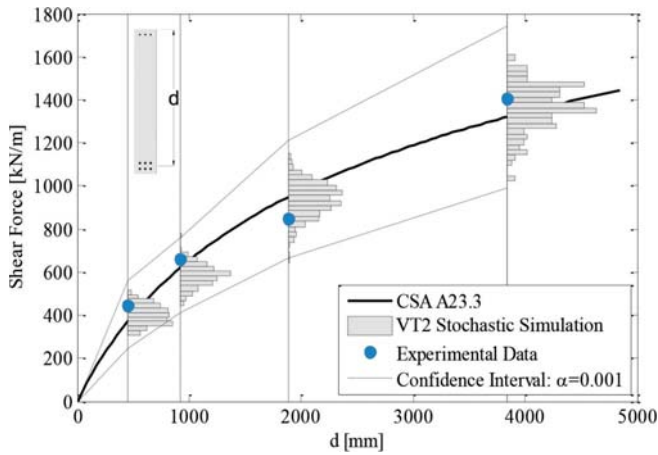


Fig. 7—Comparison of stochastic simulation results, experimental results, and CSA A23.3. (Note: 1.0 mm = 0.04 in.; 1 kN = 0.225 kip.)

DISCUSSION

Two sets of reliability analyses were conducted. The first set evaluates the reliability of each specimen. The second treats the reliability of the specimens as a whole, in comparison with the CSA code. The specimens being analyzed are not part of a real structure, and thus they have no real definition of live load and dead load. It is for this reason that the loading ratio is specified. However, if the dead load is simply the self-weight of the specimens, then the ratio between nominal strength and self-weight decreases as the depth of the beam increases. Thus, when calculating the reliability of a given structural element with unknown dead and live loads, a different approach is required. Both methods considered rely on codified calculations of the nominal resistance of the member. For this analysis, the CSA code is used for the nominal resistance.

For a typical reliability analysis, the load statistics are based on the load combinations and the loads acting on the global structure. In the case of this study, as no specific live load can be defined for any of the specimens, an approach similar to Szerszen and Nowak³⁸ is adopted. The loading ratio, ψ , is defined as

$$\psi = D/(D + L) \quad (10)$$

If the loading ratio ranges from 0 to 1, the live load can be determined based on the dead load and the loading ratio or vice versa. The live load can be divided into two categories: the sustained live load and the transient live load. The sustained live load is also referred to as the load at any arbitrary point in time, while the structure is under normal occupancy. The transient live load represents conditions when the load is at a maximum. Loading statistics compiled from the literature can be found in Szerszen and Nowak.³⁸

Method 1—With the first method, the dead load is considered an unknown value, the nominal resistance is considered to be known, and the loading ratio is specified. In the case of this study, CSA load factors and material resistance factors are assumed. Thus, the load factors for dead and live load

are taken as 1.25 and 1.5, respectively. With respect to the resistance factor, the beams are shear-critical and contain no transverse reinforcement. As such, the resistance factor for the structural element can be taken as the material resistance factor for concrete (0.65). The limit state function can be described as

$$1.25D + 1.5L \leq 0.65R_n \quad (11)$$

where D and L are the specified dead and live loads, respectively; and R_n is the nominal resistance.

Substituting Eq. (10) into (11) and solving for the dead load yields

$$D = \frac{0.65R_n}{1.25 + 1.5 \frac{1 - \psi}{\psi}} \quad (12)$$

Szerszen and Nowak³⁸ note that a realistic loading ratio for beams ranges from 0.3 and 0.7; however, a loading ratio between 0 and 1 is used for this analysis.

The mean values of the dead and live loads (μ_D and μ_L) are defined as the product between the bias factors (λ_D and λ_L) and the nominal values (D and L)

$$\mu_D = \lambda_D D \text{ and } \mu_L = \lambda_L L \quad (13)$$

This first method is useful for comparing the reliability between the selected specimens because the nominal resistance and statistical parameters for each are known. The unknown loading parameters on the tested specimens can be determined to calculate code acceptable loading.

Method 2—With the second method, a dead load is assumed. The required nominal resistance is then computed by solving Eq. (11) for the nominal resistance

$$R_n = \frac{0.65}{\left(1.25 + 1.5 \frac{1 - \psi}{\psi}\right)} D \quad (14)$$

The nominal resistance can then be used to determine the statistical parameters of the member resistance curve. To do so, a model that relates the nominal resistance and the mean resistance is required. A bias factor is generally used to relate the mean resistance with the nominal resistance. The statistical resistance model used for this analysis is taken as

$$R = R_n \times M \times P \times F \quad (15)$$

where M is the material property parameter; $R_n \times M$ is taken as the results of the stochastic simulation; P is the professional factor; and F is the fabrication factor.

The statistical properties of R can be calculated as

$$\mu_R = \lambda_R R_n \quad (16)$$

$$\sigma_R = V_R \mu_R \quad (17)$$

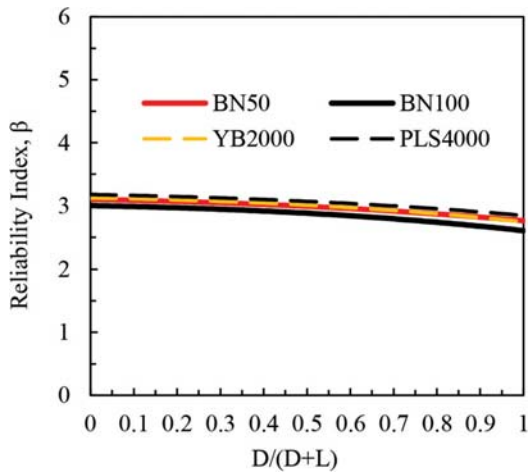


Fig. 8—Reliability index for CSA-A23.3.

where μ_R and σ_R are the mean and standard deviation of the resistance; λ_R is the bias factor for the resistance; and V_R is the coefficient of variation.

The bias factor and the coefficient of variation can be determined as

$$\lambda_R = \lambda_M \times \lambda_P \times \lambda_F \quad (18)$$

$$V_R = \sqrt{(V_M)^2 + (V_P)^2 + (V_F)^2} \quad (19)$$

where $\lambda_M = 1.142$ is the bias factor for M calculated in Table 4; $\lambda_P = 1.106$ is the bias factor for P , calculated previously in Section *VecTor2 Professional Factor*; $\lambda_F = 1.004$ is the bias factor for F calculated based on thickness measurements performed by Quach³⁷ for Specimen PLS4000. The mean value of the thickness measurements was 251 mm (9.88 in.), and the nominal thickness was 250 mm (9.84 in.). Thus, $\lambda_F = 251/250 = 1.004$; $V_M = 0.103$ is the coefficient of variation for M calculated in Table 4; $V_P = 0.174$ is the coefficient of variation for P calculated in Eq. (9); and $V_F = 0.01$ is the coefficient of variation for F calculated based on thickness measurements performed by Quach³⁷ for Specimen PLS4000 through a series of sleeves cast into the specimen as part of the formwork.

For cases where there are multiple load combinations, Method 2 can be employed where the maximum nominal resistance R_n , is computed from each load combination. The resulting statistical parameters then use Turkstra's Rule for load combinations (Nowak and Collins³⁹).

With the statistical parameters for the loading and the resistance, the reliability index can be calculated for either method using Eq. (5). Both methods produce identical results for reliability, regardless of the assumed dead load, if the statistical parameters for the resistance are identical. The second method has the advantage of being able to consider multiple load combinations.

The reliability for each specimen is calculated using the first method and the CSA code predictions for the nominal resistance. The results of the reliability analysis are shown in Fig. 8. The CSA reliability for all specimens is almost identical. This is in part due to the similar material factor,

bias factors, and coefficients of variation, but also due to the professional factor. The variability of the professional factor dominates the variability of the resistance model, and thus all bias factors and coefficients of variation for each specimen trend toward the same value. The average reliability index for the CSA code calculations is 2.96. This is below the target reliability index of $\beta_T = 3.5$ suggested by Szerszen and Nowak.³⁸ It suggests that in the case of shear-critical reinforced concrete elements without skin reinforcement and containing no transverse reinforcement, their design may not meet the required reliability. This is particularly concerning in deep concrete mat foundations, which act as large, deep flexural elements which are often designed without transverse reinforcement, the subject of the PLS4000 study by Quach.³⁷

CONCLUSIONS

Several sampling techniques for stochastic simulation were successfully implemented in the NLFEA program VecTor2. The software was expanded to perform Monte Carlo simulations, Latin hypercube simulation, random field generation, and correlated sampling (both MC and LHS).

The professional factor for VecTor2, as well as for any other analytical tool, is unique to the structure type being analyzed. In this work, the professional factor statistics were obtained by comparing the experimental to predicted ratios of the peak loads for a large number of deterministic tests involving shear-critical beams containing no transverse reinforcement. The process for creating finite element models in VecTor2 was successfully automated. From a study involving a database of 318 beams tested, the professional factor was found to be normally distributed with a mean value of 1.106 and a coefficient of variation of 0.174. This professional factor was incorporated into the reliability analysis.

The implemented stochastic simulation tools were used to assess the reliability of shear-critical reinforced concrete beams without transverse reinforcement. Four beams from the "Toronto Size Effect Series" were selected, and a stochastic simulation for each beam was completed. The results of the stochastic simulation were then used in a reliability analysis for the CSA A23.3¹⁸ code. For the specimens investigated in this study, the analysis results showed that there was no influence of the size effect on the predicted reliability for the CSA A23.3¹⁸ code. However, the average reliability index for the CSA A23.3¹⁸ code, calculated to be 2.96, is below the target reliability index of 3.5. This suggests that further investigation is required to assess the load factors and safety factors for this class of structure, particularly with respect to the shear strength of deep concrete mat foundations, transfer slabs, or outrigger slabs, which may be designed in absence of transverse shear reinforcement.

RECOMMENDATIONS FOR FUTURE WORK

Some limitations and deficiencies were identified, suggesting the following aspects are in need of further research.

1. There has not been a Canadian update to the statistical descriptions of concrete strength in approximately 20 years. It is recommended that cylinders be collected from across Canada from multiple concrete suppliers to create a database

of concrete cylinder strengths. Additionally, tests for the tangent modulus of elasticity and tensile strength of concrete should be included in the study.

2. A similar reliability study for the ACI 318-19 code is recommended as a future study.

3. From an analytical perspective, shortcomings in the current implementations need to be addressed. First, it is recommended that correlated Latin hypercube sampling be added to the alternate method for simulating random fields. This will lead to improved sampling accuracy for smaller sample sizes. Second, it is recommended that cross-correlated random fields be implemented such that the direct correlation between compressive random fields and tensile random fields is not used.

4. Additional stochastic properties should be added to the current software formulation. Stochastic variables for the steel reinforcing bar area, the depth of steel reinforcement, the thickness of structural elements, and the remaining physical dimensions should be incorporated into stochastic analysis methods.

5. To aid in usability, stochastic simulation post processing should be incorporated within a postprocessor.

6. Lastly, nonlinear finite element analysis tools (specifically, program VecTor2) should be expanded to deterministically and stochastically assess deteriorated structures including corrosion of steel reinforcement. A tool that can assess the reliability of deteriorated infrastructure could prove invaluable in ensuring that the structures most at risk receive appropriate funding.

AUTHOR BIOS

Mark D. Hunter is an Associate Principal at Quinn Dressel Associates in Toronto, ON, Canada. He received his BSc from the University of Waterloo, Waterloo, ON, Canada, and his MSc from the University of Toronto, Toronto, ON, Canada. His research interests include stochastic finite element analysis of reinforced concrete structures.

Anca C. Ferche is an Assistant Professor in the Department of Civil, Architectural, and Environmental Engineering at the University of Texas at Austin, Austin, TX. She received her PhD from the University of Toronto in 2020. Her research interests include performance assessment and analysis of reinforced concrete structures, concrete deterioration mechanisms, and rehabilitation of structures.

Frank J. Vecchio, F.ACI, is a Professor in the Department of Civil and Mineral Engineering at the University of Toronto. He is a past member of Joint ACI-ASCE Committees 441, Reinforced Concrete Columns, and 447, Finite Element Analysis of Reinforced Concrete Structures; and is a recipient of the following ACI awards: Structural Research Award (1998), Structural Engineering Award (1999), Wason Medal (2011), Joe Kelley Award (2016), and Arthur J. Boase Award (2020). His research interests include advanced constitutive modeling and analysis of reinforced concrete, assessment and rehabilitation of structures, and response to extreme loads.

ACKNOWLEDGMENTS

The authors would like to acknowledge IC-IMPACTS and NSERC for funding support provided to this project. The authors would also like to acknowledge P. Quach, E. Bentz, and M. Collins for their generous sharing of information related to PLS4000, which was being done concurrently with this work. Lastly, the authors wish to acknowledge K.-H. Reineck for sharing his database of shear-critical concrete beam tests. Without the generous contributions of the aforementioned, the present work could not have been completed.

REFERENCES

1. Vecchio, F. J., "Disturbed Stress Field Model for Reinforced Concrete: Formulation," *Journal of Structural Engineering*, ASCE, V. 126, No. 9, 2000, pp. 1070-1077. doi: 10.1061/(ASCE)0733-9445(2000)126:9(1070)
2. Nowak, A. S., and Szerszen, M. M., "Calibration of Design Code for Buildings (ACI 318): Part 1—Statistical Models for Resistance," *ACI Structural Journal*, V. 100, No. 3, May-June 2003, pp. 378-382.
3. Rakoczy, A., and Nowak, A., "Resistance Model of Lightweight Concrete Members," *ACI Materials Journal*, V. 110, No. 1, Jan.-Feb. 2013, pp. 99-109.
4. Bartlett, F. M., "Canadian Standards Association Standard A23.3-04 Resistance Factor for Concrete in Compression," *Canadian Journal of Civil Engineering*, V. 34, No. 9, 2007, pp. 1029-1037. doi: 10.1139/107-034
5. Mirza, S. A.; MacGregor, J. G.; and Hatzinikolas, M., "Statistical Descriptions of Strength of Concrete," *Journal of the Structural Division*, V. 105, No. 6, 1979, pp. 1021-1037. doi: 10.1061/JSDEAG.0005161
6. Bartlett, F. M., and MacGregor, J. G., "Statistical Analysis of the Compressive Strength of Concrete in Structures," *ACI Materials Journal*, V. 93, No. 2, Mar.-Apr. 1996, pp. 158-168.
7. Unanwa, C., and Mahan, M., "Statistical Analysis of Concrete Compressive Strengths for California Highway Bridges," *Journal of Performance of Constructed Facilities*, ASCE, V. 28, No. 1, 2014, pp. 157-167. doi: 10.1061/(ASCE)CF.1943-5509.0000404
8. Habibi, S., "Finite Element Modelling of Corrosion Damaged Reinforced Concrete Structures," MSc thesis, University of Toronto, 2017.
9. Ferche, A. C.; Panesar, D. K.; Sheikh, S. A.; and Vecchio, F. J., "Toward Macro-Modeling of Alkali-Silica Reaction-Affected Structures," *ACI Structural Journal*, V. 114, No. 5, Sept.-Oct. 2017, pp. 1121-1129. doi: 10.14359/51700778
10. Mu, R.; Miao, C.; Luo, X.; and Sun, W., "Interaction between Loading, Freeze-Thaw Cycles, and Chloride Salt Attack of Concrete with and without Steel Fiber Reinforcement," *Cement and Concrete Research*, V. 32, No. 7, 2002, pp. 1061-1066. doi: 10.1016/S0008-8846(02)00746-9
11. Ramsay, R. J.; Mirza, S. A.; and MacGregor, J. G., "Monte Carlo Study of Short Time Deflections of Reinforced Concrete Beams," *ACI Journal Proceedings*, V. 76, No. 8, 1979, pp. 897-918.
12. Mirza, S. A., and MacGregor, J. G., "Probabilistic Study of Strength of Reinforced Concrete Members," *Canadian Journal of Civil Engineering*, V. 9, No. 3, 1982, pp. 431-448. doi: 10.1139/182-053
13. Mirza, S. A., "Monte Carlo Simulation of Dispersions in Composite Steel-Concrete Column Strength Interaction," *Engineering Structures*, V. 20, No. 1-2, 1998, pp. 97-104. doi: 10.1016/S0141-0296(97)00049-7
14. Choi, B.; Scanlon, A.; and Johnson, P. A., "Monte Carlo Simulation of Immediate and Time-Dependent Deflections of Reinforced Concrete Beams and Slabs," *ACI Structural Journal*, V. 101, No. 5, Sept.-Oct. 2004, pp. 633-641.
15. Vincent, T.; Ozbakkaloglu, T.; Seracino, R.; and Kaggwa, W., "Influence of Variations in Concrete Material Properties on the Serviceability of Reinforced and Prestressed Concrete Flexural Members," *Engineering Structures*, V. 33, No. 1, 2011, pp. 99-106. doi: 10.1016/j.engstruct.2010.09.022
16. Ning, C., and Li, B., "Probabilistic Development of Shear Strength Model for Reinforced Concrete Squat Walls," *Earthquake Engineering & Structural Dynamics*, V. 46, No. 6, 2017, pp. 877-897. doi: 10.1002/eqe.2834
17. Wong, P. S.; Vecchio, F. J.; and Trommels, H., "VecTor2 & FormWorks User's Manual," *Technical Report*, Department of Civil Engineering, University of Toronto, 2013.
18. Canadian Standards Association, "Design of Concrete Structures (CSA A23.3-14)," CSA, Mississauga, ON, Canada, 2014.
19. ACI Committee 318, "Building Code Requirements for Structural Concrete (ACI 318-19) and Commentary (ACI 318R-19)," American Concrete Institute, Farmington Hills, MI, 2019, 624 pp.
20. Collins, M. P.; Bentz, E. C.; Quach, P. T.; and Proestos, G. T., "The Challenge of Predicting the Shear Strength of Very Thick Slabs," *Concrete International*, V. 37, No. 11, Nov. 2015, pp. 29-37.
21. Melchers, R. E., *Structural Reliability Analysis and Prediction*, second edition, Wiley, Chichester, UK, 1999.
22. Mirza, S. A., and MacGregor, J. G., "Variability of Mechanical Properties of Reinforcing Bars," *Journal of the Structural Division*, V. 105, No. 5, 1979, pp. 921-937. doi: 10.1061/JSDEAG.0005146
23. Graham, C., and Talay, D., *Stochastic Simulation and Monte Carlo Methods: Mathematical Foundations of Stochastic Simulation*, Springer, New York, 2013.
24. Marsaglia, G., and Tsang, W. W., "A Simple Method for Generating Gamma Variables," *ACM Transactions on Mathematical Software*, V. 26, No. 3, 2000, pp. 363-372. doi: 10.1145/358407.358414

25. Hunter, M. D., "Towards Stochastic Finite Element Analysis of Reinforced Concrete Structures," MSc thesis, University of Toronto, Toronto, ON, Canada, 2016.
26. McKay, M. D.; Beckman, R. J.; and Conover, W. J., "A Comparison of Three Methods for Selecting Values of Input Variables in the Analysis of Output from a Computer Code," *Technometrics*, V. 21, No. 2, 1979, pp. 239-245.
27. Olsson, A.; Sandberg, G.; and Dahlblom, O., "On Latin Hypercube Sampling for Structural Reliability Analysis," *Structural Safety*, V. 25, No. 1, 2003, pp. 47-68. doi: 10.1016/S0167-4730(02)00039-5
28. Vořechovský, M., and Novák, D., "Simulation of Random Fields for Stochastic Finite Element Analysis," *Proceedings, ICOSSAR*, Rotterdam, the Netherlands, 2005, pp. 2545-2552.
29. Choi, S.; Canfield, R. A.; and Grandhi, R. V., "Estimation of Structural Reliability for Gaussian Random Fields," *Structure and Infrastructure Engineering*, V. 2, No. 3-4, 2006, pp. 161-173. doi: 10.1080/15732470600590192
30. Vecchio, F. J.; Lai, D.; Shim, W.; and Ng, J., "Disturbed Stress Field Model for Reinforced Concrete: Validation," *Journal of Structural Engineering*, ASCE, V. 127, No. 4, 2001, pp. 350-358. doi: 10.1061/(ASCE)0733-9445(2001)127:4(350)
31. Reineck, K.; Bentz, E. C.; Fitik, B. F.; Kuchma, D. A.; and Bayrak, O., "ACI-DAfStb Database of Shear Tests on Slender Reinforced Concrete Beams without Stirrups," *ACI Structural Journal*, V. 110, No. 5, Sept.-Oct. 2013, pp. 867-876.
32. Comité Euro-International du Béton, "Model Code for Concrete Structures: CEB-FIP International Recommendations," third edition, CEB-FIP, Paris, France, 1978, 348 pp.
33. Vecchio, F. J., and Collins, M. P., "The Modified Compression-Field Theory for Reinforced Concrete Elements Subjected to Shear," *ACI Journal Proceedings*, V. 83, No. 2, Mar.-Apr. 1986, pp. 219-231.
34. Bentz, E. C., "Sectional Analysis of Reinforced Concrete Members," doctoral thesis, University of Toronto, Toronto, ON, Canada, 2000.
35. Podgorniak-Stanik, B. A., "The Influence of Concrete Strength, Distribution of Longitudinal Reinforcement, Amount of Transverse Reinforcement, and Member Size on Shear Strength of Reinforced Concrete Members," master's thesis, University of Toronto, Toronto, ON, Canada, 1998.
36. Yoshida, Y., "Shear Reinforcement for Large Lightly Reinforced Concrete Members," master's thesis, University of Toronto, Toronto, ON, Canada, 2000.
37. Quach, P., "Understanding and Safely Predicting the Shear Response of Large-Scale Reinforced Concrete Structures," master's thesis, University of Toronto, Toronto, ON, Canada, 2016.
38. Szerszen, M. M., and Nowak, A. S., "Calibration of Design Code for Buildings (ACI 318): Part 2—Reliability Analysis and Resistance Factors," *ACI Structural Journal*, V. 100, No. 3, May-June 2003, pp. 383-391.
39. Nowak, A. S., and Collins, K. R., *Reliability of Structures*, McGraw Hill, Boston, MA, 2000.
40. Saatci, S., and Vecchio, F. J., "Effects of Shear Mechanisms on Impact Behavior of Reinforced Concrete Beams," *ACI Structural Journal*, V. 106, No. 1, Jan.-Feb. 2009, pp. 78-86.
41. Ferche, A. C., and Vecchio, F. J., "Influence of Crack Spacing Parameters on MCFT Calculations of the Behaviour of Shear-Critical Beams without Transverse Reinforcement," *Proceedings, Denis Mitchell Symposium on Developments in Shear and Torsion Design, Seismic Design and Concrete Material*, Montreal, QC, Canada, 2017.